FRONTIERS OF PHYSICS

RESEARCH ARTICLE
Volume 18 / Issue 6 / 61302 / 2023

Quantum simulation of Hofstadter butterfly with synthetic gauge fields on two-dimensional superconducting-qubit lattices

Wei Feng[1], Dexi Shao[1], Guo-Qiang Zhang[1], Qi-Ping Su[1], Jun-Xiang Zhang[2,†], Chui-Ping Yang[1,‡]

1 School of Physics, Hangzhou Normal University, Hangzhou 311121, China
2 School of Physics, Zhejiang University, Hangzhou 310027, China
Corresponding authors. E-mail: †junxiang_zhang@zju.edu.cn, ‡yangcp@hznu.edu.cn
Received March 22, 2023; accepted June 6, 2023

ABSTRACT

Motivated by recent realizations of two-dimensional (2D) superconducting-qubit lattices, we propose a protocol to simulate Hofstadter butterfly with synthetic gauge fields in superconducting circuits. Based on the existing 2D superconducting-qubit lattices, we construct a generalized Hofstadter model on zigzag lattices, which has a fractal energy spectrum similar to the original Hofstadter butterfly. By periodically modulating the resonant frequencies of qubits, we engineer a synthetic gauge field to mimic the generalized Hofstadter Hamiltonian. A spectroscopic method is used to demonstrate the Hofstadter butterfly from the time evolutions of experimental observables. We numerically simulate the dynamics of the system with realistic parameters, and the results show a butterfly spectrum clearly. Our proposal provides a promising way to realize the Hofstadter butterfly on the latest 2D superconducting-qubit lattices and will stimulate the quantum simulation of novel properties induced by magnetic fields in superconducting circuits.

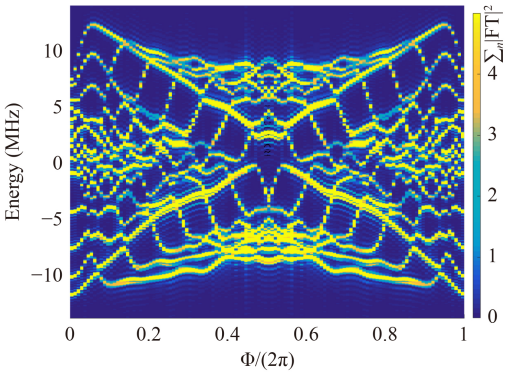

Keywords quantum simulation, superconducting circuits, superconducting qubit, quantum computation

1 Introduction

Quantum simulation is promising to efficiently solve many-body problems of complex quantum systems [1]. In general, there are two strategies in quantum simulation: one is digital quantum simulation based on quantum logic gates, and the other is analog quantum simulation which directly mimics the target Hamiltonian with controllable quantum systems [2, 3]. Compared with digital quantum simulation, analog quantum simulation is not universal, but it has higher tolerance level of errors [4]. For many problems that require only qualitative but not quantitative results, analog quantum simulations can give meaningful results even if they are affected by quantum decoherence. Experimental demonstrations of analog quantum simulation have already been performed on a number of platforms, such as optical lattices and trapped ions [5–7]. It is expected that special-purpose analog quantum simulators for some practical tasks will be realized in the near future.

Hofstadter butterfly is a famous fractal energy spectrum that was first predicted in theory by Hofstadter in 1976 [8]. The original Hofstadter butterfly was found in a system of electrons on a two-dimensional (2D) square lattice exposed to a perpendicular magnetic field. In

Higher Education Press

arXiv: 2306.11245
https://doi.org/10.1007/s11467-023-1319-x

general, the experimental observation requires that the characteristic length of the magnetic field is comparable to the lattice constant. The estimated strength of the magnetic field required to observe the Hofstadter butterfly for conventional solid-state crystals is on the order of 10^4 T, which is too high to be experimentally realized. One way to overcome this problem is to use graphene superlattices with larger lattice constant, which can reduce the required strength of magnetic fields [9–13]. On the other hand, the Hofstadter butterfly can be demonstrated by analog quantum simulation with synthetic gauge fields in artificial systems. When a charged particle moves on a closed loop under a magnetic field, its wave function will obtain a geometric phase related to the magnetic flux through the loop. Synthesizing a gauge field can be equated to trying to make a neutral particle acquire a non-trivial phase after one revolution around a closed loop. The synthesis of gauge fields in artificial quantum systems is of great importance to simulate magnetic effects including the Hofstadter butterfly. In recent years, the implementation of synthetic gauge fields in artificial controllable systems (e.g., cold atoms [14–16], cavity QEDs [17, 18], superconducting circuits [19–27]) and related quantum simulations have become a hot research area. Simultaneously, many protocols have been proposed to mimic the Hofstadter model with synthetic gauge fields in platforms such as optical lattices with ultracold atoms [28], trapped ions [29], and polaritonic systems [30]. In experiments [31, 32], researchers provided evidence that they have engineered the Hofstadter Hamiltonian, but the fractal energy spectrum could not be measured directly.

Superconducting circuits provide an excellent platform to perform quantum simulations due to their flexibility and scalability [33–42]. Recently, significant technological breakthroughs have been made in superconducting circuits. In particular, the experimental realization of 2D architectures, such as square [43–47], zigzag [48–50], ladder [51], and hyperbolic [52] lattices, makes it possible to simulate 2D lattice models using superconducting circuits. For the simulation of Hofstadter butterfly on 2D superconducting-qubit lattices, a qubit flip interaction is analog to the hopping of an electron. The key problem is how to create the synthetic gauge fields. One method for engineering the synthetic gauge field in superconducting circuits is based on the periodic modulation of interaction strengths [19–24], also named as parametric process, which however can not be applied on the recent 2D superconducting-qubit lattices [43–51]. By contrast, another method is based on the periodic modulation of on-site energies, which is easy to be realized for superconducting transmon qubits and has been adopted in the protocols of generating synthetic gauge fields on ladder lattices [25–27]. Although a reduced 1D Harper Hamiltonian [53, 54] has been simulated using a chain of superconducting qubits [55], the simulation of 2D Hofstadter Hamiltonian in superconducting circuits is still lacking.

In this paper, motivated by experimental realizations of 2D lattices in superconducting qubit circuits [43–52], we theoretical study the Hofstadter butterfly with synthetic gauge fields on 2D superconducting-qubit lattices. It is difficult to realize a uniform gauge field on the existing square lattices of superconducting qubits. Therefore, we generalize the original Hofstadter model from square lattices to zigzag lattices, and we find a fractal energy spectrum similar to the original Hofstadter butterfly. To mimic the generalized Hofstadter Hamiltonian, we design a modulation scheme based on the zigzag superconducting-qubit lattices previously reported. By modulating the qubit frequencies with appropriate initial phases and amplitudes, we engineer an artificial magnetic field and realize the Hofstadter Hamiltonian on zigzag superconducting-qubit lattices. Further, we resolve the fractal energy spectrum from time evolutions of experimental observables. We also numerically simulate the evolution process based on the original time-dependent Hamiltonian of the superconducting-qubit lattice. With a group of realistic parameters, a simulated spectrum resembles a butterfly obviously, which confirms our scheme is feasible with existing superconducting-qubit lattices.

This paper is organized as follows. In Section 2, we introduce the Hofstadter model on zigzag lattices and show its fractal energy spectrum. In Section 3, we present the modulation scheme for generating artificial gauge fields and mimicking the Hofstadter Hamiltonian on zigzag superconducting-qubit lattices. In Section 4, we give a method to detect the fractal energy spectrum from time evolutions of experimental observables and discuss the experimental feasibility with numerical simulations. Finally, we make a conclusion in Section 5.

2 Model

We consider a zigzag spin lattice, which is experimentally achievable in superconducting circuits [48–50]. As shown in Fig. 1, each spin is coupled to four nearest neighbors and the coupling coefficients are complex numbers with spatially varying phases. The system can be described by a Hofstadter-like Hamiltonian (assuming $\hbar = 1$)

$$H = J\sum_n \left[\mathrm{e}^{\mathrm{i}n\phi}\sigma_n^+\sigma_{n+2}^- + \mathrm{e}^{-\mathrm{i}(n+1)\phi}\sigma_n^+\sigma_{n+1}^-\right] + \mathrm{H.c.}, \tag{1}$$

where σ_n^+ (σ_n^-) is the raising (lowering) operator of the nth spin, and J represents the coupling strength between spins. This Hamiltonian commutes with the total excitation $\sum_n \sigma_n^+\sigma_n^-$ and the system is energy-conserving. In the single-excitation manifold, i.e., only

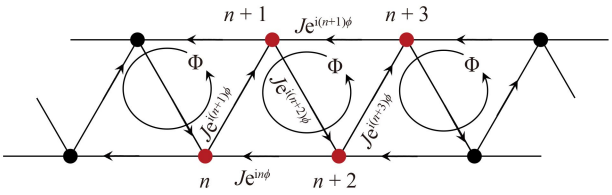

Fig. 1 A zigzag spin chain with nearest-neighbor interactions. Arrows between spins denote the complex-valued interactions shown in Eq. (1). The shown setup leads to constant fluxes $\Phi = 3\phi$ through rhombic unit cells.

one spin is up and all others are down, this spin-flip model maps onto a free hopping model of a charged particle in a lattice under magnetic fields. For a triangle formed by three spins n, $n+1$, and $n+2$, the associated magnetic flux $(3n+3)\,\phi$ is spatially dependent. However, the flux through rhombic unit cells, as shown in Fig. 1, is a constant: $\Phi = 3\phi$. When $\Phi/(2\pi)$ is rational, i.e., $\Phi/(2\pi) = p/q$ with p and q two coprime integers, the Hamiltonian is of period q. In the momentum space, the dispersion $E(k)$ has q bands with the wave vector k restricted to a magnetic Brillouin zone $[-\pi/q, \pi/q]$. By Fourier transform $\sigma_n^+ = \sum_{k,v} \mathrm{e}^{-\mathrm{i}n(k+v\phi)}\sigma_{k,v}^+$, with v the band index, the Hamiltonian is transformed to $H = \sum_k H_k$, where

$$H_k = J\sum_v \left[\mathrm{e}^{\mathrm{i}(k+v\phi)} + \mathrm{e}^{-\mathrm{i}2(k+v\phi)}\right]\sigma_{k,v}^+\sigma_{k,v+1}^- + \mathrm{H.c.}. \tag{2}$$

In contrast to the cosine modulation of the on-site energies in the original Harper Hamiltonian [53–55]

$$H_{\mathrm{Harper}} = J\sum_n (\sigma_n^+\sigma_{n+1}^- + \sigma_{n+1}^+\sigma_n^- + 2\cos(n\Phi)\,\sigma_n^+\sigma_n^-), \tag{3}$$

the coupling strengths between the neighbouring bands in H_k periodically vary with the magnetic flux Φ as

$$\left|\mathrm{e}^{\mathrm{i}(k+v\phi)} + \mathrm{e}^{-\mathrm{i}2(k+v\phi)}\right| = \sqrt{2+2\cos(3k+v\Phi)}. \tag{4}$$

We solve the model by diagonalizing an $N \times N$ matrix with N the number of the spins. The eigenenergy spectrum versus the magnetic flux is plotted in Fig. 2(a). For comparison, an original Hofstadter butterfly obtained by diagonalizing H_{Harper} in Eq. (3) is plotted in Fig. 2(b). One can see that the fractal energy spectrum of the zigzag lattice is very similar to the original Hofstadter butterfly, despite small difference at, e.g., $\Phi = 0$. The small difference of the energy spectra can be clearly explained through the Hamiltonian matrices of H_k and H_{Harper}. When $\Phi = 0$, the matrix trace of H_{Harper} is $2N$ (in unit of J) while the matrix trace of H_k is zero, which is confirmed by eigenenergy data shown in Fig. 2.

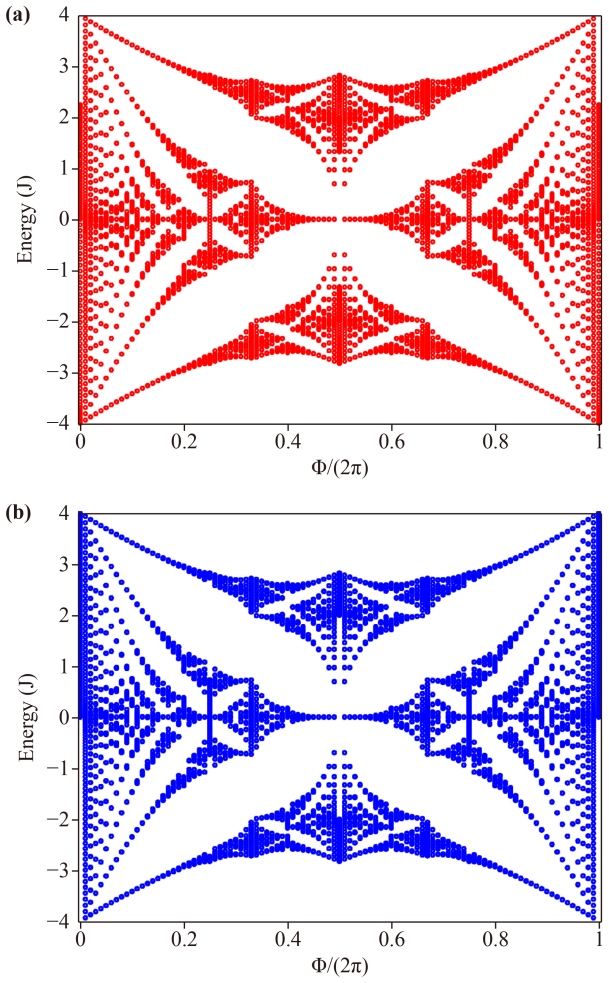

Fig. 2 Fractal energy spectra: the energy eigenvalues are plotted as a function of the flux Φ in the single spin-flip subspace. **(a)** The fractal energy spectrum of the generalized model on the zigzag lattice. **(b)** The original Hofstadter butterfly on the square lattice. We adopt periodic boundary conditions in a system of $N = 300$ spins.

3 Synthetic gauge field

The coupling strength between superconducting qubits is usually a real number due to time-reversal symmetry. We can realize the effective complex-valued coupling in Eq. (1) by modulating resonant frequencies of qubits. The original Hamiltonian of N frequency-tunable qubits arranged in a zigzag lattice is [48–50]

$$H_o = \sum_n \omega_n(t)\,\sigma_n^+\sigma_n^- + g\sum_n \left(\sigma_{n+1}^+\sigma_n^- + \sigma_{n+2}^+\sigma_n^-\right) + \mathrm{H.c.}, \tag{5}$$

where σ_n^+ (σ_n^-) denotes the raising (lowering) operator of the nth qubit Q_n, and g is the original real-valued coupling strength between qubits. The resonant frequency of Q_n is periodically modulated according to

$$\omega_n(t) = \bar{\omega}_n + \varepsilon_n \cos(\nu_n t + \theta_n), \tag{6}$$

where $\bar{\omega}_n$ is the central frequency, and ε_n, ν_n, and θ_n are the modulation amplitude, frequency, and initial phase, respectively. Under the modulation, each qubit generate a bunch of equally spaced sidebands with a spacing equalling to the modulation frequency ν_n [56–58]. We set $\nu_1 = \Delta_{13}$, $\nu_2 = \Delta_{12}$, $\nu_3 = \Delta_{23}$ and repeat the settings $\bar{\omega}_n = \bar{\omega}_j$ and $\nu_n = \nu_j$ for $n \equiv j \pmod 3$ with $j = 1, 2, 3$ (see Fig. 3), where $\Delta_{mn} = \bar{\omega}_m - \bar{\omega}_n$. In these settings, sideband transitions with tunable qubit-qubit interactions can be implemented. Under the condition of large detuning $|\Delta_{mn}| \gg g$, high-frequency oscillating terms can be neglected and the effective Hamiltonian in the interaction picture can be written as [58]

$$H_{\text{eff}} = \sum_n (J_{n,n+1}\sigma_{n+1}^{+}\sigma_n^{-} + J_{n+2,n}\sigma_n^{+}\sigma_{n+2}^{-}) + \text{H.c.}, \tag{7}$$

where the effective coupling strengths $J_{n,n+1}$ and $J_{n+2,n}$ are given by

$$J_{n,n+1} = \begin{cases} g\mathcal{J}_0(\alpha_n)\mathcal{J}_1(\alpha_{n+1})\,\mathrm{e}^{\mathrm{i}\theta_{n+1}}, & n \equiv 1 \pmod 3, \\ g\mathcal{J}_0(\alpha_n)\mathcal{J}_{-1}(\alpha_{n+1})\,\mathrm{e}^{-\mathrm{i}\theta_{n+1}}, & n \equiv 3 \pmod 3, \end{cases} \tag{8}$$

$$J_{n+2,n} = \begin{cases} g\mathcal{J}_0(\alpha_{n+2})\mathcal{J}_{-1}(\alpha_n)\,\mathrm{e}^{-\mathrm{i}\theta_n}, & n \equiv 1 \pmod 3, \\ g\mathcal{J}_0(\alpha_{n+2})\mathcal{J}_1(\alpha_n)\,\mathrm{e}^{\mathrm{i}\theta_n}, & n \equiv 2, 3 \pmod 3, \end{cases} \tag{9}$$

with $\mathcal{J}_m(\alpha_n)$ being the mth-order Bessel function of the first kind. Both magnitudes and phases of the above effective coupling strengths can be conveniently tuned by changing $\alpha_n = \varepsilon_n/\nu_n$ and θ_n. If we set

$$\theta_n = \begin{cases} \pi - n\phi, & n \equiv 1 \pmod 3, \\ n\phi, & n \equiv 2, 3 \pmod 3, \end{cases} \tag{10}$$

and all α_n to be the same value, the effective Hamiltonian H_{eff} becomes the Hofstadter-like Hamiltonian in Eq. (1).

In summary, based on the original Hamiltonian of the superconducting-qubit system in Eq. (5), we periodically modulate the resonant frequency of each qubit according to Eq. (6). By finely setting the modulation parameters $\bar{\omega}_n$, ε_n, ν_n, and θ_n, we approximatively obtain the Hofstadter-like Hamiltonian in Eq. (1) under the large-detuning condition $|\Delta_{mn}| \gg g$. The parameter setting shown above is specially designed for synthesizing the uniform gauge field in the Hofstadter-like Hamiltonian. Other kinds of synthetic gauge fields can be engineered by changing the parameter setting.

4 Observing fractal energy spectrum

The energy spectrum of an interacting many-body system can be revealed by probing the system's dynamical responses to perturbations [55, 59, 60]. If the eigenenergies

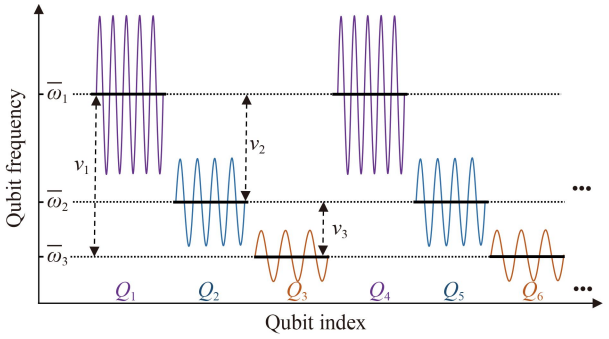

Fig. 3 Frequency setting and modulation scheme for synthesizing the complex-valued interaction. The resonant frequency of each qubit is periodically modulated around its central frequency $\bar{\omega}_n$ (black solid line). For sideband transitions, the modulation frequency is specially setted with $\nu_1 = \bar{\omega}_1 - \bar{\omega}_3$, $\nu_2 = \bar{\omega}_1 - \bar{\omega}_2$, and $\nu_3 = \bar{\omega}_2 - \bar{\omega}_3$. Latter qubits repeat the settings $\bar{\omega}_n = \bar{\omega}_j$ and $\nu_n = \nu_j$ where $n \equiv j \pmod 3$ with $j = 1, 2, 3$.

$\{E_j\}$ and the corresponding eigenstates $\{|\psi_j\rangle\}$ of a fixed Hamiltonian are given, the state time evolution of the system can be expressed as

$$|\Psi(t)\rangle = \sum_j c_j \mathrm{e}^{-\mathrm{i}E_j t}|\psi_j\rangle, \tag{11}$$

where $c_j = \langle\psi_j|\Psi(0)\rangle$, and $|\Psi(0)\rangle$ is the initial state of the system. In turn, if the time evolution is known, its Fourier transform can in principle reveal the eigenenergies. To realize this scheme in reality, we need to choose a group of appropriate initial states and observables. For an operator $\hat{q} = \sum_{j,j'} q_{j,j'}|\psi_j\rangle\langle\psi_{j'}|$, its expectation value is

$$\langle\hat{q}\rangle = \langle\Psi(t)|\hat{q}|\Psi(t)\rangle = \sum_{j,j'} q_{j,j'} c_j c_{j'}^{*} \mathrm{e}^{-\mathrm{i}(E_j - E_{j'})t}, \tag{12}$$

which indicates that the Fourier transforms of observable results can only reveal eigenenergy differences $E_j - E_{j'}$. In our qubit model, the Hofstadter Butterfly is presented in the single-excitation subspace $\{|\psi_n\rangle \equiv |000\ldots1_n\ldots00\rangle\}$, and the associated single-excitation eigenenergies E_j for $j = 1, 2, \ldots, N$ can be calibrated by selecting the ground state $(|\psi_0\rangle \equiv |0\rangle^{\otimes N})$ energy $E_0 \equiv 0$ as a reference. To do that, the state of the qubit system should have overlaps $(c_j, c_{j'}^{*})$ both with the ground state $|\psi_0\rangle$ and single-excitation states $|\psi_j\rangle$, and the selected operator should have corresponding matrix element $q_{j,0}$. Therefore, a suitable initial state should be in superposition of $|\psi_0\rangle$ and $|\psi_j\rangle$, and a suitable operator should relate to $|\psi_j\rangle\langle\psi_0|$.

Next, we verify the above scheme by numerical simulations based on the original time-dependent Hamiltonian H_o given in Eq. (5). Initially, we prepare the nth qubit in the state $(|0\rangle + |1\rangle)/\sqrt{2}$ and all other qubits in the state $|0\rangle$, i.e., the system is in the state $(|\psi_0\rangle + |\psi_n\rangle)/\sqrt{2}$. We simulate the time evolution of the state of the

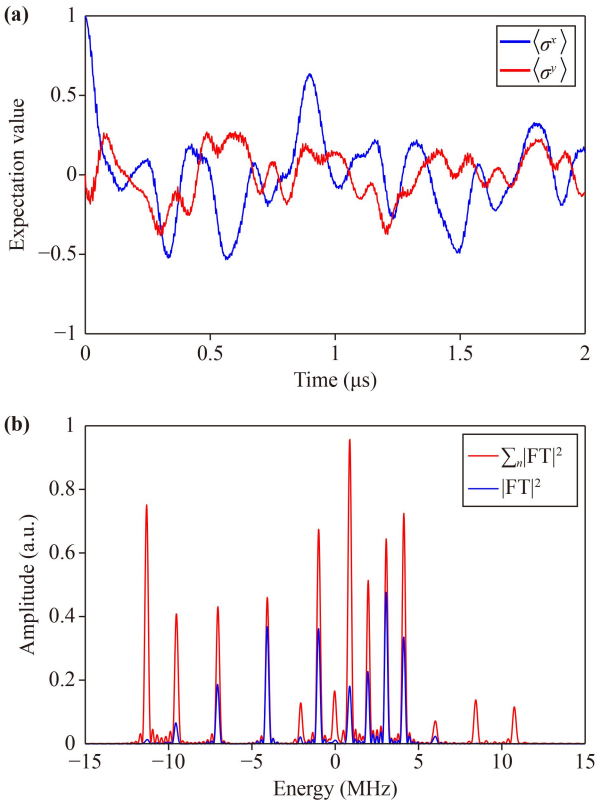

Fig. 4 Spectroscopic signatures of the interacting multi-qubit system. **(a)** Typical curves of time evolutions of $\langle\sigma_n^x\rangle$ and $\langle\sigma_n^y\rangle$. The results are simulated using the original Hamiltonian H_o with the initial state $(|\psi_0\rangle + |\psi_n\rangle)/\sqrt{2}$ and the qubit number $N = 14$. Relevant parameters are chosen as $g/(2\pi) = 10\,\text{MHz}$, $\nu_1/(2\pi) = 250\,\text{MHz}$, $\nu_2/(2\pi) = 150\,\text{MHz}$, $\nu_3/(2\pi) = 100\,\text{MHz}$, $\phi/(2\pi) = 1/120$, and $\alpha_n = 1$. The relaxation and pure dephasing times of the superconducting qubits are $T_1 = 20\,\mu\text{s}$ and $T_2^* = 2\,\mu\text{s}$, respectively. **(b)** Squared Fourier transform (FT) amplitudes of $\langle\sigma_n^x\rangle + \text{i}\langle\sigma_n^y\rangle = 2\langle\sigma_n^-\rangle$. The peaks in the FT results correspond to the eigenenergies of the system. The blue curve is the FT result of one set of data shown in (a), which only shows part of the eigenenergies. The red curve is the summation of the FT results of $\langle\sigma_n^-\rangle$ for $n \in \{1, 2, ..., 14\}$, which shows all 14 eigenenergies with 14 peaks.

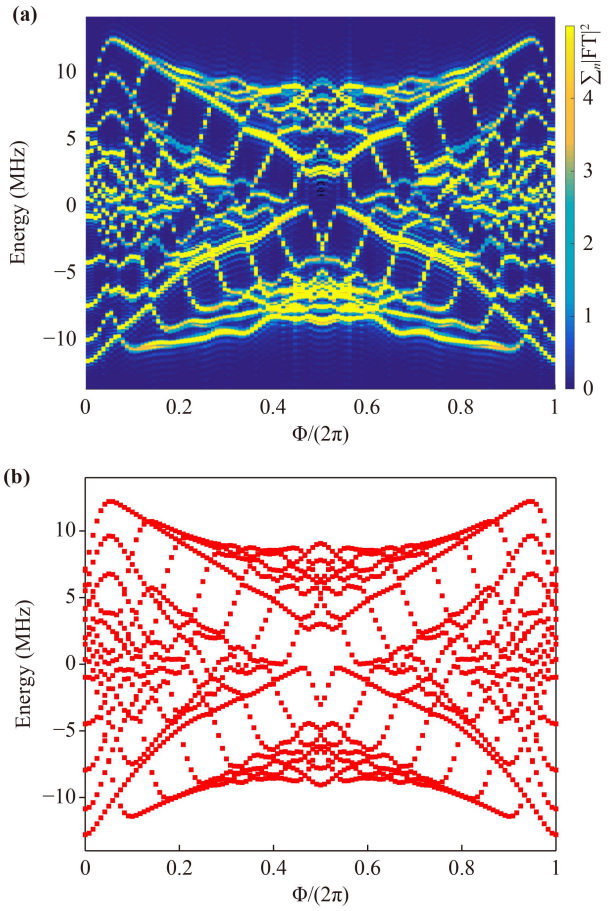

Fig. 5 **(a)** Quantum simulation of Hofstadter butterfly on the superconducting-qubit lattice. Data similar to Fig. 4(b), summation of squared Fourier transform amplitudes are shown for 120 values of magnetic flux $\Phi/(2\pi)$ ranging from 0 to 1. For each $\Phi/(2\pi)$ value, time evolution of $\langle\sigma_n^-\rangle$ is simulated using the original Hamiltonian H_o with the same parameters as in Fig. 4(a). **(b)** As a comparison, theoretical Hofstadter butterfly from model Hamiltonian H is shown with the same conditions that $N = 14$ and open boundary.

system under the periodical modulation described in Section 3 by considering the qubit dissipation. We also calculate the expectation value of the operator σ_n^-. Although σ_n^- is non-Hermitian and cannot be measured directly, it can be inferred from observables σ_n^x and σ_n^y as $\langle\sigma_n^x\rangle + \text{i}\langle\sigma_n^y\rangle = 2\langle\sigma_n^-\rangle$. Typical time evolutions of $\langle\sigma_n^x\rangle$ and $\langle\sigma_n^y\rangle$ in the simulation are shown in Fig. 4(a), and the result of Fourier transform of the corresponding expectation value $\langle\sigma_n^-\rangle$ is shown in Fig. 4(b). For the simulated system containing N qubits, there should be N single-excitation eigenenergies. From the blue curve in Fig. 4(b), we can see part of eigenenergies in the time-domain spectrum. To resolve all the eigenenergies, we vary n from 1 to N, which makes the initial states form a complete basis. Then every eigenstate certainly has some overlap with one of the initial states and hence its corresponding eigenenergy can be detected.

To obtain the fractal spectrum versus the magnetic flux, we vary $\Phi/(2\pi)$ from 0 to 1 with 120 different values. For each $\Phi/(2\pi)$ value, we place the nth qubit in the state $(|0\rangle + |1\rangle)/\sqrt{2}$, simulate the evolution of $\langle\sigma_n^-\rangle$, and vary n from 1 to N. Using the spectroscopy shown above, we obtain a fractal energy spectrum of the Hofstadter butterfly shown in Fig. 5(a), where the qubit number is $N = 14$. Despite there are only 14 sites in the simulated lattice, the overall energy spectrum still has a butterfly-like appearance. To verify the accuracy of the energy spectrum based on Fourier transforms, we diagonalize the 14×14 matrix of the Hamiltonian in Eq. (1), and show the theoretical results in Fig. 5(b). The similarity between these two energy spectra indicates that our scheme for simulating Hofstadter butterfly with

synthetic gauge fields is effective. Note that there is small difference between Figs. 5(a) and (b), especially in the smallest eigenenergy when $\Phi = 0$. The tiny deviations of the Fourier transform spectrum from the theoretical results arise mainly from the large-detuning approximation in obtaining the effective Hamiltonian in Eq. (7).

The above numerical simulations, which use the original time-dependent Hamiltonian and consider the qubit dissipation, are performed based on QuTiP [61, 62]. Because the Lindblad-master-equation simulation of the 14-qubit system is beyond our computer's memory capability, we use a Monte Carlo approach which is based on the state vector instead of the density matrix. In the simulations, we adopt the experimental achievable parameters of zigzag superconducting-qubit lattices [48–50]. In addition, the similar frequency modulations have already been used in the experiments [48, 58, 63]. Therefore, our scheme is experimentally realizable with the existing superconducting-qubit lattices.

5 Conclusion

In summary, we propose an experimentally feasible scheme to demonstrate fractal energy spectra on 2D superconducting-qubit lattices with synthetic gauge fields. A generalized Hofstadter model on zigzag lattices is studied by employing the superconducting-qubit lattices previously realized in experiments. The model exhibits a fractal energy spectrum similar to the original Hofstadter butterfly. We design a modulation scheme of qubit frequencies to generate synthetic gauge fields and mimic the generalized Hofstadter Hamiltonian on the zigzag superconducting-qubit lattices. We present a method to detect the fractal energy spectrum from time evolutions of experimental observables. With experimental feasible parameters, our simulation results clearly demonstrate a Hofstadter butterfly. The proposal provides a promising way to study Hofstadter problems on the latest 2D superconducting-qubit lattices. Our work will stimulate the quantum simulation of novel properties induced by magnetic fields in superconducting circuits.

Declarations The authors declare that they have no competing interests and there are no conflicts.

Acknowledgements This work was supported by the National Natural Science Foundation of China (Grant Nos. 12204139, U20A2076, 12204138, 12205069, 11774076, and U21A20436) and the Key-Area Research and Development Program of Guangdong Province (Grant No. 2018B030326001).

References

1. R. P. Feynman, Simulating physics with computers, *Int. J. Theor. Phys.* 21(6–7), 467 (1982)
2. I. M. Georgescu, S. Ashhab, and F. Nori, Quantum simulation, *Rev. Mod. Phys.* 86(1), 153 (2014)
3. I. Buluta and F. Nori, Quantum simulators, *Science* 326(5949), 108 (2009)
4. S. Somaroo, C. H. Tseng, T. F. Havel, R. Laflamme, and D. G. Cory, Quantum simulations on a quantum computer, *Phys. Rev. Lett.* 82(26), 5381 (1999)
5. J. Simon, W. S. Bakr, R. Ma, M. E. Tai, P. M. Preiss, and M. Greiner, Quantum simulation of antiferromagnetic spin chains in an optical lattice, *Nature* 472(7343), 307 (2011)
6. I. Bloch, J. Dalibard, and S. Nascimbene, Quantum simulations with ultracold quantum gases, *Nat. Phys.* 8(4), 267 (2012)
7. K. Kim, M. S. Chang, S. Korenblit, R. Islam, E. E. Edwards, J. K. Freericks, G. D. Lin, L. M. Duan, and C. Monroe, Quantum simulation of frustrated Ising spins with trapped ions, *Nature* 465(7298), 590 (2010)
8. D. R. Hofstadter, Energy levels and wave functions of Bloch electrons in rational and irrational magnetic fields, *Phys. Rev. B* 14(6), 2239 (1976)
9. C. R. Dean, L. Wang, P. Maher, C. Forsythe, F. Ghahari, Y. Gao, J. Katoch, M. Ishigami, P. Moon, M. Koshino, T. Taniguchi, K. Watanabe, K. L. Shepard, J. Hone, and P. Kim, Hofstadter's butterfly and the fractal quantum Hall effect in moiré superlattices, *Nature* 497(7451), 598 (2013)
10. L. A. Ponomarenko, R. V. Gorbachev, G. L. Yu, D. C. Elias, R. Jalil, A. A. Patel, A. Mishchenko, A. S. Mayorov, C. R. Woods, J. R. Wallbank, M. Mucha-Kruczynski, B. A. Piot, M. Potemski, I. V. Grigorieva, K. S. Novoselov, F. Guinea, V. I. Fal'ko, and A. K. Geim, Cloning of Dirac fermions in graphene superlattices, *Nature* 497(7451), 594 (2013)
11. B. Hunt, J. D. Sanchez-Yamagishi, A. F. Young, M. Yankowitz, B. J. LeRoy, K. Watanabe, T. Taniguchi, P. Moon, M. Koshino, P. Jarillo-Herrero, and R. C. Ashoori, Massive Dirac fermions and Hofstadter butterfly in a van der Waals heterostructure, *Science* 340(6139), 1427 (2013)
12. Q. S. Wu, J. Liu, Y. Guan, and O. V. Yazyev, Landau levels as a probe for band topology in graphene moiré superlattices, *Phys. Rev. Lett.* 126(5), 056401 (2021)
13. A. V. Rozhkov, A. O. Sboychakov, A. L. Rakhmanov, and F. Nori, Electronic properties of graphene-based bilayer systems, *Phys. Rep.* 648, 1 (2016)
14. J. Dalibard, F. Gerbier, G. Juzeliunas, and P. Öhberg, Colloquium: Artificial gauge potentials for neutral atoms, *Rev. Mod. Phys.* 83(4), 1523 (2011)
15. V. Galitski and I. B. Spielman, Spin–orbit coupling in quantum gases, *Nature* 494(7435), 49 (2013)
16. F. Gerbier and J. Dalibard, Gauge fields for ultracold atoms in optical superlattices, *New J. Phys.* 12(3), 033007 (2010)
17. J. Cho, D. G. Angelakis, and S. Bose, Fractional quantum Hall state in coupled cavities, *Phys. Rev. Lett.* 101(24), 246809 (2008)
18. R. O. Umucalılar and I. Carusotto, Artificial gauge field for photons in coupled cavity arrays, *Phys. Rev. A* 84(4), 043804 (2011)

19. P. Roushan, C. Neill, A. Megrant, Y. Chen, R. Babbush, R. Barends, B. Campbell, Z. Chen, B. Chiaro, A. Dunsworth, A. Fowler, E. Jeffrey, J. Kelly, E. Lucero, J. Mutus, P. J. J. O'Malley, M. Neeley, C. Quintana, D. Sank, A. Vainsencher, J. Wenner, T. White, E. Kapit, H. Neven, and J. Martinis, Chiral ground-state currents of interacting photons in a synthetic magnetic field, *Nat. Phys.* 13(2), 146 (2017)
20. J. Koch, A. A. Houck, K. L. Hur, and S. M. Girvin, Time-reversal-symmetry breaking in circuit-QED-based photon lattices, *Phys. Rev. A* 82(4), 043811 (2010)
21. A. Nunnenkamp, J. Koch, and S. M. Girvin, Synthetic gauge fields and homodyne transmission in Jaynes–Cummings lattices, *New J. Phys.* 13(9), 095008 (2011)
22. D. Marcos, P. Rabl, E. Rico, and P. Zoller, Superconducting circuits for quantum simulation of dynamical gauge fields, *Phys. Rev. Lett.* 111(11), 110504 (2013)
23. Y. P. Wang, W. L. Yang, Y. Hu, Z. Y. Xue, and Y. Wu, Detecting topological phases of microwave photons in a circuit quantum electrodynamics lattice, *npj Quantum Inf.* 2(1), 16015 (2016)
24. Z. H. Yang, Y. P. Wang, Z. Y. Xue, W. L. Yang, Y. Hu, J. H. Gao, and Y. Wu, Circuit quantum electrodynamics simulator of flat band physics in a Lieb lattice, *Phys. Rev. A* 93(6), 062319 (2016)
25. H. Alaeian, C. W. S. Chang, M. V. Moghaddam, C. M. Wilson, E. Solano, and E. Rico, Creating lattice gauge potentials in circuit QED: The bosonic Creutz ladder, *Phys. Rev. A* 99(5), 053834 (2019)
26. Y. J. Zhao, X. W. Xu, H. Wang, Y. X. Liu, and W. M. Liu, Vortex–Meissner phase transition induced by a two-tone-drive-engineered artificial gauge potential in the fermionic ladder constructed by superconducting qubit circuits, *Phys. Rev. A* 102(5), 053722 (2020)
27. X. Guan, Y. L. Feng, Z. Y. Xue, G. Chen, and S. T. Jia, Synthetic gauge field and chiral physics on two-leg superconducting circuits, *Phys. Rev. A* 102(3), 032610 (2020)
28. D. Jaksch and P. Zoller, Creation of effective magnetic fields in optical lattices: The Hofstadter butterfly for cold neutral atoms, *New J. Phys.* 5, 56 (2003)
29. T. Graß, C. Muschik, A. Celi, R. W. Chhajlany, and M. Lewenstein, Synthetic magnetic fluxes and topological order in one-dimensional spin systems, *Phys. Rev. A* 91(6), 063612 (2015)
30. R. Banerjee, T. C. H. Liew, and O. Kyriienko, Realization of Hofstadter's butterfly and a one-way edge mode in a polaritonic system, *Phys. Rev. B* 98(7), 075412 (2018)
31. M. Aidelsburger, M. Atala, M. Lohse, J. T. Barreiro, B. Paredes, and I. Bloch, Realization of the Hofstadter Hamiltonian with ultracold atoms in optical lattices, *Phys. Rev. Lett.* 111(18), 185301 (2013)
32. H. Miyake, G. A. Siviloglou, C. J. Kennedy, W. C. Burton, and W. Ketterle, Realizing the Harper Hamiltonian with laser-assisted tunneling in optical lattices, *Phys. Rev. Lett.* 111(18), 185302 (2013)
33. J. Q. You and F. Nori, Atomic physics and quantum optics using superconducting circuits, *Nature* 474(7353), 589 (2011)
34. X. Gu, A. F. Kockum, A. Miranowicz, Y. Liu, and F. Nori, Microwave photonics with superconducting quantum circuits, *Phys. Rep.* 718–719, 1 (2017)
35. J. Clarke and F. K. Wilhelm, Superconducting quantum bits, *Nature* 453(7198), 1031 (2008)
36. P. J. J. O'Malley, R. Babbush, I. D. Kivlichan, J. Romero, J. R. McClean, et al., Scalable quantum simulation of molecular energies, *Phys. Rev. X* 6(3), 031007 (2016)
37. K. Xu, J. J. Chen, Y. Zeng, Y. R. Zhang, C. Song, W. Liu, Q. Guo, P. Zhang, D. Xu, H. Deng, K. Huang, H. Wang, X. Zhu, D. Zheng, and H. Fan, Emulating many-body localization with a superconducting quantum processor, *Phys. Rev. Lett.* 120(5), 050507 (2018)
38. W. Feng, G. Q. Zhang, Q. P. Su, J. X. Zhang, and C. P. Yang, Generation of Greenberger–Horne–Zeilinger states on two-dimensional superconducting-qubit lattices via parallel multiqubit-gate operations, *Phys. Rev. Appl.* 18(6), 064036 (2022)
39. Q. P. Su, Y. Zhang, L. Bin, and C. P. Yang, Efficient scheme for realizing a multiplex-controlled phase gate with photonic qubits in circuit quantum electrodynamics, *Front. Phys.* 17(5), 53505 (2022)
40. T. Liu, B. Q. Guo, Y. H. Zhou, J. L. Zhao, Y. L. Fang, Q. C. Wu, and C. P. Yang, Transfer of quantum entangled states between superconducting qubits and microwave field qubits, *Front. Phys.* 17(6), 61502 (2022)
41. Q. P. Su, H. Zhang, and C. P. Yang, Transferring quantum entangled states between multiple single-photonstate qubits and coherent-state qubits in circuit QED, *Front. Phys.* 16(6), 61501 (2021)
42. T. Liu, Z. F. Zheng, Y. Zhang, Y. L. Fang, and C. P. Yang, Transferring entangled states of photonic cat-state qubits in circuit QED, *Front. Phys.* 15(2), 21603 (2020)
43. F. Arute, K. Arya, R. Babbush, D. Bacon, J. C. Bardin, et al., Quantum supremacy using a programmable superconducting processor, *Nature* 574(7779), 505 (2019)
44. M. Gong, S. Wang, C. Zha, M. C. Chen, H. L. Huang, et al., Quantum walks on a programmable two-dimensional 62-qubit superconducting processor, *Science* 372(6545), 948 (2021)
45. Y. Wu, W. S. Bao, S. Cao, F. Chen, M. C. Chen, et al., Strong quantum computational advantage using a superconducting quantum processor, *Phys. Rev. Lett.* 127(18), 180501 (2021)
46. X. Zhang, W. Jiang, J. Deng, K. Wang, J. Chen, P. Zhang, W. Ren, H. Dong, S. Xu, Y. Gao, F. Jin, X. Zhu, Q. Guo, H. Li, C. Song, A. V. Gorshkov, T. Iadecola, F. Liu, Z. X. Gong, Z. Wang, D. L. Deng, and H. Wang, Digital quantum simulation of Floquet symmetry protected topological phases, *Nature* 607(7919), 468 (2022)
47. W. Ren, W. Li, S. Xu, K. Wang, W. Jiang, F. Jin, X. Zhu, J. Chen, Z. Song, P. Zhang, H. Dong, X. Zhang, J. Deng, Y. Gao, C. Zhang, Y. Wu, B. Zhang, Q. Guo, H. Li, Z. Wang, J. Biamonte, C. Song, D. L. Deng, and H. Wang, Experimental quantum adversarial learning with programmable superconducting qubits, *Nat. Comput. Sci.* 2(11), 711 (2022)
48. W. Liu, W. Feng, W. Ren, D. W. Wang, and H. Wang,

Synthesizing three-body interaction of spin chirality with superconducting qubits, *Appl. Phys. Lett.* 116(11), 114001 (2020)

49. W. Ren, W. Liu, C. Song, H. Li, Q. Guo, Z. Wang, D. Zheng, G. S. Agarwal, M. O. Scully, S. Y. Zhu, H. Wang, and D. W. Wang, Simultaneous excitation of two noninteracting atoms with time-frequency correlated photon pairs in a superconducting circuit, *Phys. Rev. Lett.* 125(13), 133601 (2020)
50. Q. Guo, C. Cheng, H. Li, S. Xu, P. Zhang, Z. Wang, C. Song, W. Liu, W. Ren, H. Dong, R. Mondaini, and H. Wang, Stark many-body localization on a superconducting quantum processor, *Phys. Rev. Lett.* 127(24), 240502 (2021)
51. Y. Ye, Z. Y. Ge, Y. Wu, S. Wang, M. Gong, Y. R. Zhang, Q. Zhu, R. Yang, S. Li, F. Liang, J. Lin, Y. Xu, C. Guo, L. Sun, C. Cheng, N. Ma, Z. Y. Meng, H. Deng, H. Rong, C. Y. Lu, C. Z. Peng, H. Fan, X. Zhu, and J. W. Pan, Propagation and localization of collective excitations on a 24-qubit superconducting processor, *Phys. Rev. Lett.* 123(5), 050502 (2019)
52. A. J. Kollár, M. Fitzpatrick, and A. A. Houck, Hyperbolic lattices in circuit quantum electrodynamics, *Nature* 571(7763), 45 (2019)
53. P. G. Harper, Single band motion of conduction electrons in a uniform magnetic field, *Proc. Phys. Soc. A* 68(10), 874 (1955)
54. K. K. Das and J. Christ, Realizing the Harper model with ultracold atoms in a ring lattice, *Phys. Rev. A* 99(1), 013604 (2019)
55. P. Roushan, C. Neill, J. Tangpanitanon, V. M. Bastidas, A. Megrant, R. Barends, Y. Chen, Z. Chen, B. Chiaro, A. Dunsworth, A. Fowler, B. Foxen, M. Giustina, E. Jeffrey, J. Kelly, E. Lucero, J. Mutus, M. Neeley, C. Quintana, D. Sank, A. Vainsencher, J. Wenner, T. White, H. Neven, D. G. Angelakis, and J. Martinis, Spectroscopic signatures of localization with interacting photons in superconducting qubits, *Science* 358(6367), 1175 (2017)
56. F. Beaudoin, M. P. da Silva, Z. Dutton, and A. Blais, First-order sidebands in circuit QED using qubit frequency modulation, *Phys. Rev. A* 86(2), 022305 (2012)
57. J. D. Strand, M. Ware, F. Beaudoin, T. A. Ohki, B. R. Johnson, A. Blais, and B. L. T. Plourde, First-order sideband transitions with flux-driven asymmetric transmon qubits, *Phys. Rev. B* 87, 220505(R) (2013)
58. X. Li, Y. Ma, J. Han, T. Chen, Y. Xu, W. Cai, H. Wang, Y. P. Song, Z. Y. Xue, Z. Q. Yin, and L. Sun, Perfect quantum state transfer in a superconducting qubit chain with parametrically tunable couplings, *Phys. Rev. Appl.* 10(5), 054009 (2018)
59. C. Senko, J. Smith, P. Richerme, A. Lee, W. C. Campbell, and C. Monroe, Coherent imaging spectroscopy of a quantum many-body spin system, *Science* 345(6195), 430 (2014)
60. P. Jurcevic, P. Hauke, C. Maier, C. Hempel, B. P. Lanyon, R. Blatt, and C. F. Roos, Spectroscopy of interacting quasiparticles in trapped ions, *Phys. Rev. Lett.* 115(10), 100501 (2015)
61. J. R. Johansson, P. D. Nation, and F. Nori, QuTiP: An open-source Python framework for the dynamics of open quantum systems, *Comput. Phys. Commun.* 183(8), 1760 (2012)
62. J. R. Johansson, P. D. Nation, and F. Nori, QuTiP2: A Python framework for the dynamics of open quantum systems, *Comput. Phys. Commun.* 184(4), 1234 (2013)
63. D. W. Wang, C. Song, W. Feng, H. Cai, D. Xu, H. Deng, H. Li, D. Zheng, X. Zhu, H. Wang, S. Y. Zhu, and M. O. Scully, Synthesis of antisymmetric spin exchange interaction and chiral spin clusters in superconducting circuits, *Nat. Phys.* 15(4), 382 (2019)